

## REMOTE SENSING OF POLAR REGIONS USING LASER ALTIMETRY

Beata M. Csatho and Toni A. Schenk  
Byrd Polar Research Center and Department of Geodetic Sciences and Surveying  
The Ohio State University  
Columbus, OH 43210  
email: csatho@ohglas.mps.ohio-state.edu

Robert H. Thomas  
Code YS, NASA HQ  
Washington, DC 20546

William B. Krabill  
Laboratory of Hydrospheric Processes  
NASA/Goddard Space Flight Center  
Wallops Island, VA 23337

Commission I, Working Group 3

**KEY WORDS:** Mapping, DEM/DTM, Data Integration, Laser Altimetry System, Change\_Detection

### ABSTRACT

The vast ice sheets of Antarctica and Greenland cover almost 10% of the Earth's land surface. Together with sea ice they have a significant influence on local and global climate. Moreover, the mass balance of the polar ice is a sensitive indicator of global climate changes. There is a growing concern that some ice fluctuation may occur at a rapid rate with an associated effect on the global sea level. Thus it is imperative to monitor the ice sheets on a global scale, assess their mass balance, and predict their future behavior. This paper reports about studies that have been carried out to derive DEMs and topographic maps from airborne laser altimetry data. NASA's laser scanning system covers a 130 to 200 m wide swath with a set of overlapping spirals. The densely distributed data, together with an accuracy of 10 to 20 cm, lends itself into deriving accurate DEMs and into generating topographic maps that contain interesting morphological details necessary to analyze the surface characteristic as well as changes. The position of the system is determined by kinematic GPS. A ring-laser gyro inertial navigation system provides attitude information. Independent attitude information is obtained from three widely separated GPS antennas on the airplane, suitable to control the INS drift. For the experiments described in this paper, five parallel flight strips have been bridged together to form a 4 km wide and 400 km long DEM. In order to check the accuracy, an independent DEM was derived by photogrammetric methods. A detailed analysis confirmed a strong agreement between the two DEMs. Also the topography depicted by the two approaches is very similar.

### 1. INTRODUCTION

The vast ice sheets of Antarctica and Greenland cover almost 10% of the Earth's land surface. Together with sea ice they have a significant influence on local and global climate. Moreover, the mass balance of polar ice masses is a sensitive indicator of global climate changes. There is a growing concern that some ice fluctuation may occur at a rapid rate with an associated effect on the global sea level. Thus it is imperative to monitor the ice sheets on a global scale, assess their mass balance, and predict their future behavior.

This task can not be accomplished by using traditional, well-known and proven technologies. Ice sheets exhibit a dynamic behavior with some ice streams moving as much as 1 km per year. Their surface elevation changes throughout the year and the effect of global climate changes is superimposed on this annual cycle. Clearly, detection of long term changes requires repeat measurements for several years. Another factor to consider is the size - the area to be monitored is huge. Taking the required accuracy into account, the hostility of the area (remoteness, accessibility, weather), the picture of an enormous challenge emerges.

Laser altimetry provides a solution for precise mapping and monitoring of polar regions. In NASA's Arctic Ice Mapping

Program the Airborne Topographic Mapper (ATM) - an airborne scanning system - has been used on several missions in Greenland and the Canadian Arctic. The program can be considered as a predecessor of a satellite laser altimetry program. The Geoscience Laser Altimetry System (GLAS), currently under development, will be launched in the Earth Observation System Land Ice Altimetry (EOS ALT-L) mission in 2002.

The ATM laser scanning system covers a 130-200 m wide swath with a set of overlapping spirals, providing a dense data set along the flight lines suitable for mapping ice sheet topography to unprecedented accuracy and detail. This continuous and accurate mapping capability has major potential for mass balance studies. Although this high accuracy is achieved only along the aircraft flight lines, the resulting elevation profiles can also be used for mapping surface features, such as wind generated ripples (sastrugi), lakes, and surface undulations.

This paper reports about the studies that have been carried out to derive Digital Elevation Models (DEMs) and topographic maps from airborne laser altimetry data. After a brief description of the laser altimetry system the processing of raw data including calibration aspects and error analysis follows. The last section deals with the derivation of a DEM in the Jakobshavns drainage basin from laser altimetry data and its comparison with a photogrammetrically derived DEM.

## 2. LASER ALTIMETRY FROM SPACECRAFT

Satellite laser altimeters have been developed at NASA, to study the Earth, the Moon, and the Mars (Bufton, 1989). Vertical resolution of a few centimeters can be achieved from spacecraft by employing gain switched solid state lasers with a pulse length of 1-10 nsec. The footprint size on the surface is in the order of 50-300 m (Gardner, 1992). Because of the orbital altitude of several 100 km the precise knowledge of the pointing direction and high stability is required. For example for the GLAS system the position will be obtained from GPS, and the attitude determination will be based on stellar cameras and INS.

### 2.1 Analysis of Laser Altimetry Waveform

The range between the spacecraft and the surface is determined from the round-trip propagation time of short laser pulses. To estimate the timing performance of the laser altimeters and to derive other useful surface parameters, such as surface roughness and albedo, the knowledge of the received waveform is essential. Several factors, such as terrain variations within the laser footprint, nadir angle effects, and the curvature of the laser beam contribute to the spreading of the reflected pulse. The detected signal is also contaminated by optical and electronic noise.

In special cases, such as flat or uniformly sloped terrain, the laser altimeter's detection statistics and timing performance can be expressed in closed form (Gardner, 1992). As a complementary approach to the analytical calculations, the Goddard Laser Altimetry Simulator (Abshire et al., 1994) is suitable for evaluat-

ing the laser altimeter performance over a wide range of conditions.

The simulator uses a simplified 2-D measurement geometry (height vs. along track distance). The terrain surface is assumed to be a Lambertian reflector, and its reflectivity and height can be specified for every centimeter of the along-track distance. The surface parameters can be randomized using first and second order Markov processes. The simulator computes the waveform as it is propagated to and from the terrain surface and, after detection through the altimeter receiver. The surface elevation is estimated in the following fashion. First the coarse range is calculated as the time interval between the laser firing and the receiver's first threshold time. Then a fine range correction is computed from the waveform. Finally a correction is applied to remove the effect of the low-pass filtering in the receiver. An example of the computed waveforms is given in Figure 1. The estimated surface elevation is marked with a triangle in Figure 1.a.

The shape of the received waveform is closely related to the height distribution within the laser footprint (Bufton, 1989). For many applications, the determination of surface slope or roughness is of considerable interest. In case of horizontal, random, rough, Lambertian surfaces the surface roughness within the laser footprint can be computed from the pulse spreading. An algorithm based on the analytic solution described in (Gardner, 1992) is recommended for the estimation of sea ice surface roughness in (Csatho and Thomas, 1995b).

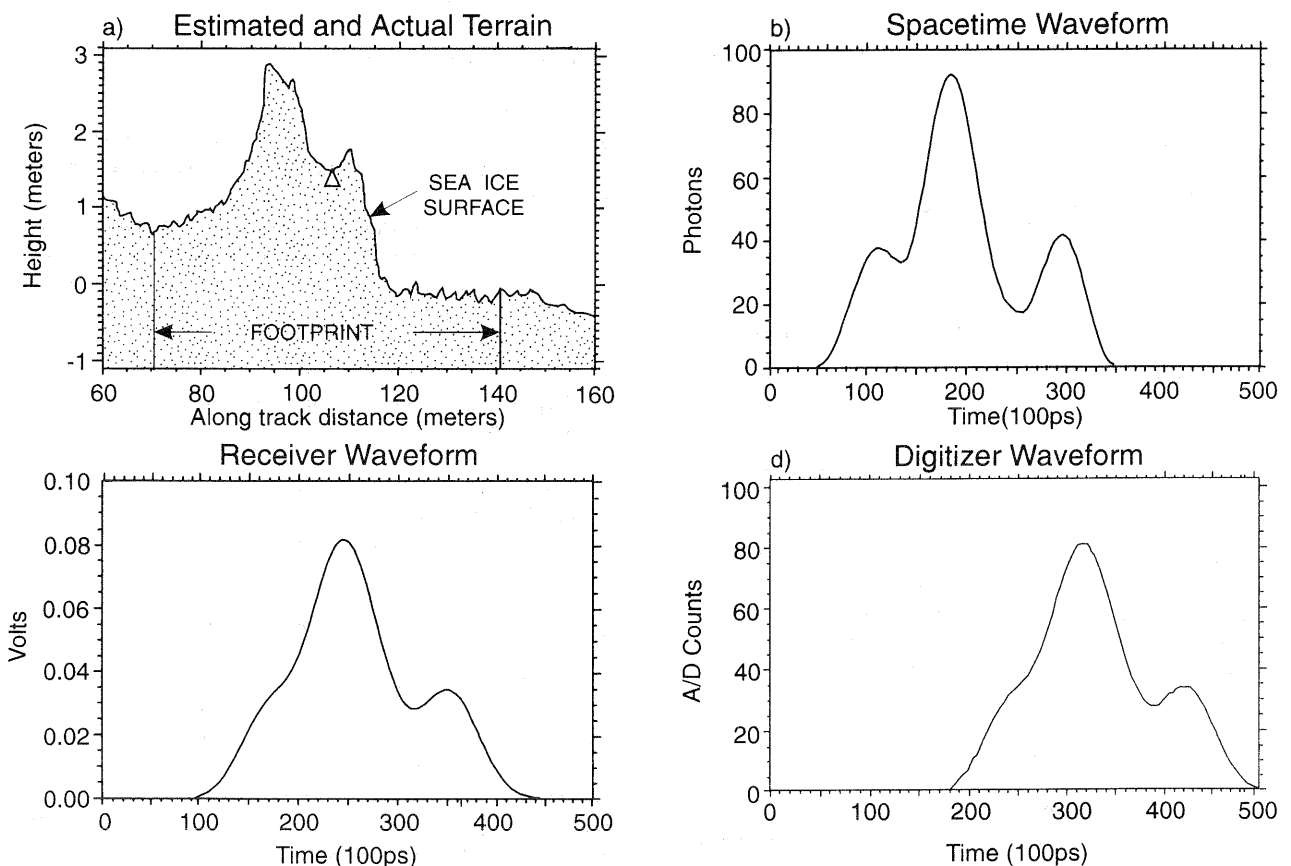


Figure 1: Simulated laser altimetry waveforms for GLAS system computed the Goddard Laser Altimetry Simulator. Surface was created from sea ice elevations measured by airborne laser altimetry.

### 3. AIRBORNE TOPOGRAPHIC MAPPER

#### 3.1 Measuring System

NASA has developed several different airborne laser systems, including the Airborne Oceanographic Lidar (Krabill and Swift 1985) and the Airborne Topographic Mapper (Krabill et al., 1995a). The latter system was developed for the sole purpose of topographic mapping, particularly for NASA's Greenland mapping program.

The laser scanner of the ATM system covers a 130-200 m wide swath with a set of overlapping spirals (Figure 1). The transmitter is a pulsed laser that operates in the visible part of the spectrum. The laser beam is directed along an oval shaped pattern with the help of a rotating mirror. At a nominal operating altitude of 400 m above ground, the laser spot on the surface has a diameter of approximately 1 m. In 1991 the scan mirror was spun at 5 Hz with a laser pulse rate of 800 Hz. The maximum along-track separation between the laser footprints was 20 m, and the cross-track separation was less than 4 m. In order to provide higher data density, the laser pulse rate and the scanner rotation rate have gradually been increased. The present system uses a laser pulse rate of 5000 Hz with 20 conical scans per second resulting a very dense data array (Figure 1).

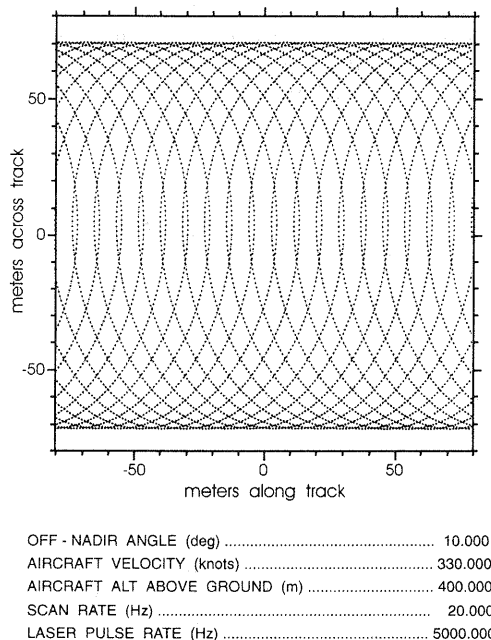


Figure 2: Scan pattern produced by ATM system (current system specifications).

The ATM system is mounted on a P-3 aircraft. The aircraft location is determined using kinematic GPS technique. The attitude information is obtained from a ring-laser gyro Inertial Navigation System. Real-time GPS data are used to provide the pilot with a visual display of the flight line and the current offset from the desired track.

#### 3.2 Calibration and Data Processing

First, the data collected by the individual sensors (laser ranging, GPS, INS) are processed independently. The various data streams are synchronized by the GPS time tags. Then they are combined to provide the 3-D coordinates of the laser footprint on the surface.

**3.2.1 Laser Ranging:** The round-trip travel time of the laser pulse between the aircraft and the surface is measured by a threshold detector. Range determination based on thresholding depends on the intensity of the received pulse. The increase in measured slant range with decreasing laser backscattering energy is often referred to as "range walk". The relationship between the residual of the true and measured range, and the received intensity is established by ground calibration. The pointing angle of the laser is determined using the rotational position of the scanning mirror obtained from a shelf mounted scan azimuth encoder.

**3.2.2 Aircraft Attitude:** is provided by the INS unit. Data from three widely separated GPS antennas on the airplane renders independent estimates of aircraft attitude for monitoring the INS drift during the flight.

**3.2.3 Aircraft Position:** is determined by using kinematic GPS technique, tracking the difference in the GPS dual frequency carrier-phase-derived ranges from a fixed receiver located over a precisely known benchmark and a mobile receiver on the aircraft.

**3.2.4 Data Integration:** The different data sets are integrated following a georeferencing scheme similar to the one suggested in (Lindenberger 1993). The mounting bias between the laser system and the INS was computed from data sets collected over flat areas such as the ocean surface in fjords. The following parameters are available after the data processing: geographic latitude, longitude, and elevation of the laser footprint (referred to WGS-84 ellipsoid), scan azimuth, pitch and roll of the aircraft, and GPS time of the measurements.

#### 3.3 Accuracy Assessment

Principle error sources are related to laser ranging, and to the determination of aircraft position and attitude. Different techniques are employed for assessing the measurement accuracy, among them:

- Overflight of runway and apron areas of staging airports previously surveyed by mobile GPS mounted on a truck.
- Overflight of profiles on the ice sheet previously surveyed by mobile GPS system mounted on a sledge towed behind a snow mobile.
- Overflight of a profile surveyed by optical leveling;
- Repeat flights and data comparison at "crossing points" of flight lines.

The results indicate that ice-surface elevations can be reliably measured by the ATM system to an RMS accuracy of 20 cm, possibly 10 cm, over baselines of more than seven hundred km (Krabill et al., 1995a).

#### 3.4 Data Thinning and Blunder Detection

The ATM data sets are very large and not easily manageable. For example in 1991 one hour flight rendered approximately 2,800,000 data points in a 400 km long swath. Spatial distribution is quite irregular with redundant data near edges, and small gaps in the middle of the swath. Outliers are caused by the reflection of the laser beam from clouds, ice fog or blowing snow, or measurement errors. A simple but efficient thinning scheme reduces the redundancy of the data sets. The recommended processing steps are as follows:

- Transformation of the ellipsoidal coordinates into a suitable projection system
- Blunder removal
- Data thinning.

Ice sheet surfaces are typically very smooth and they can be approximated by small planar patches. A patch size of 25 m was selected based on the a priori analysis of the surfaces and the scanning geometry. Because the largest distance between consecutive ellipses of the scan pattern is approximately 20 m (in 1991, much less later), every grid cell contains at least one scan line. After transforming the original ATM data into a suitable projection system, all points within a 25 meter grid cell are used to determine a best fitting plane by least squares. Blunders are removed and the elevation of the tilted plane at the cell's center is used as a representative point.

Using the centroid of the grid cell as a representative point (first order approximation) also works well. The standard deviation,  $\sigma$ , obtained in this procedure comprises two errors: observation error of the ATM data points and approximation error. It follows that larger  $\sigma$  values are to be expected on heavily crevassed areas, on rocks, on the calving front of glaciers, or over fjords with floating icebergs. Data collected during bad weather (ice fog, blowing snow, etc.) also are characterized by higher  $\sigma$  values. Examples shown in (Csatho et al., 1996) confirm the remarkably high accuracy of the ATM system. The standard deviation computed during the data thinning process is consistently below 0.15 m in smooth areas.

Greenland is quite extensively covered by ATM. The raw point elevation data are thinned and stored in the Greenland Airborne Precise Elevation Survey (GRAPES) data base. The data are available on anonymous ftp on "gdglas.gsfc.nasa.gov".

#### 4. APPLICATION OF ATM DATA FOR MAPPING

The ATM data used in this study were acquired in Greenland along the so called ERS-1 line in September 1991 (Thomas et al., 1994).

##### 4.1 Large Scale Mapping

Contour maps were generated over small areas to demonstrate the inherent potential of the ATM system for feature extraction. In order to preserve the details, the TIN model of the irregularly distributed original data points was contoured without interpolation. In Figure 3 the perspective view of such a contour map shows a gently sloping surface. The elongated, low ridges located perpendicularly to the prevailing wind direction are most likely sastrugi.

##### 4.2 Digital Elevation Model (DEM) Generation from ATM Data

DEMs are particularly suitable for further analysis of the surface. By the application of well-known techniques, such as Fourier transform, filtering, and scale-space theory, interesting features can be identified and delineated. Some experiments towards the automatic detection of lakes and other features from ATM data are presented in (Csatho et al., 1995a). DEMs also facilitate the comparison between the laser altimetry data and other elevation data sets, such as those derived from aerial

photogrammetry, Synthetic Aperture Radar (SAR) interferometry, and satellite radar and laser altimeters.

Contour interval: 0.1 m

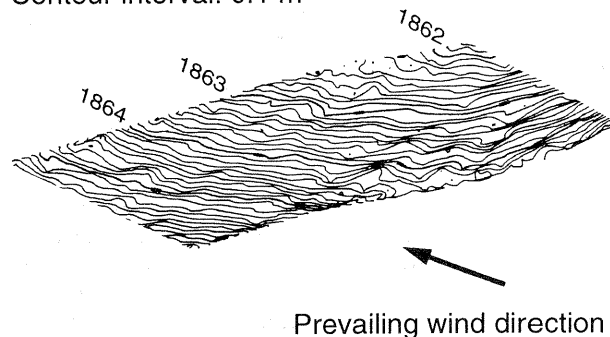


Figure 3: Perspective view of a large scale contour map generated from ATM data (swath width: 200 m).

DEMs were generated from the raw ATM using the following procedure:

- Coordinate transformation.
- Data thinning and blunder detection.
- Creation of TIN (Triangulated Irregular Network) model.
- Interactive editing and smoothing of the TIN model (optional).
- Interpolation of the TIN model.

In the examples shown in this paper the geographical coordinates were transformed into Universal Transverse Mercator (UTM) projection system. Blunders were removed by interactive editing or by applying the procedure described in Section 2.4.. The TIN models were created by Delauney triangulation and optionally smoothed by least squares. A neighborhood-based planar interpolation was used to create the DEMs and contour maps. The contour lines of the final contour maps were smoothed by a weighted average method, and drawn by B-splines. The data processing was performed on an Intergraph workstation using the MGE (Modular GIS Environment) Modeler software package from Intergraph Inc.

##### 4.3 An Example - Jakobshavns Drainage Basin, West Greenland

To obtain a DEM in the Jakobshavns drainage basin in West Greenland, five parallel ATM swaths were bridged together. The 200 m wide flight swaths are 1 km apart from each other. The elevations in the 800 m wide gaps were found by interpolation.

The velocity of the Jakobshavns glacier, which reaches 8 km/year at the floating terminus, is the highest recorded velocity of any non-surgingly glacier (e.g. Echelmeyer et al., 1991). Within the Jakobshavns drainage basin, there is considerable surface melting in summer below altitudes of about 1400 m. Fast-flowing melt streams cut into the ice, and large lakes of meltwater are formed in depressions. The lakes drain periodically through moulins at the bottom or through rivers and streams on the ice sheet surface (Thomsen et al., 1989). An abundance of the surface features and extensive knowledge acquired during years of intensive research makes the Jakobshavns drainage basin an excellent test field. The DEMs and contour maps derived from laser altimetry are described in detail in (Csatho et al., 1996).

The DEM derived from laser altimetry was checked with a DEM generated photogrammetrically. Four sets of aerial photographs (M=1:120,000) that cover a large part of the Jakobshavns drainage basin were acquired in 1985 and 1986 (Fastook et al., 1995). In our study photographs from 10 July 1985 were used. As reported in (Csatho et al., 1996) the two DEMs agree well. Figure 4 illustrates the comparison graphically. It confirms that the topography depicted by the two approaches is very similar.

For further analysis a more detailed DEM was measured. Contour lines from this DEM are superimposed on the orthophoto in Figure 4.a. No elevations could be measured in featureless areas (for example west of lake A). On the area of the ATM swath the surface elevation was accurately mapped by the laser altimetry. These elevations were used to estimate the accuracy of the photogrammetrically derived DEM. Between the parallel ATM swaths the photogrammetrically derived DEM was used to estimate the error introduced by the interpolation of the laser altimetry data. An RMS accuracy of 2.5 meter was obtained for the photogrammetry derived DEM. The laser altimetry derived DEM is very accurate over the swaths. The interpolated elevations between adjacent swaths are less accurate (maximum error is 5 m).

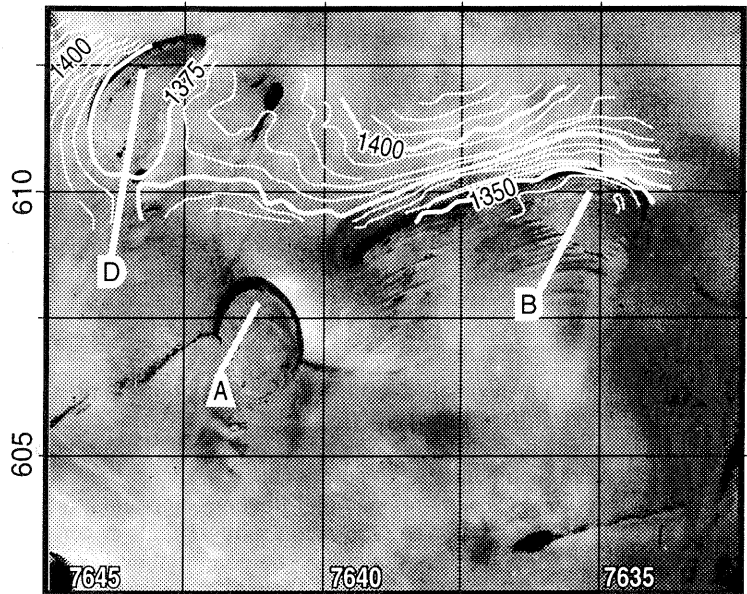
The temporal behavior of the lakes was also studied. Because the ice on the lakes melted during the photogrammetric flight mission it was possible to delineate the lakes on the orthophotos (for example Lake A in Figure 4.a). In addition, the smooth and horizontal lake surfaces can readily be identified from the laser altimetry data (for example Lake A and D in Figure 4.b and c). The comparison of the lake boundaries confirms that the larger surface depressions are tied to bedrock irregularities which means that is they do not advect with the moving ice. Analysis of the DEMs also shows that despite their proximity the lakes do not drain at the same time.

Ripples were mapped along the shorelines (for example features located west of Lake B in Figure 4.b and 4.c). These features are advecting with the moving ice downstream. Detailed maps were derived from laser altimetry data to study their shape and distribution (Csatho et al., 1996).

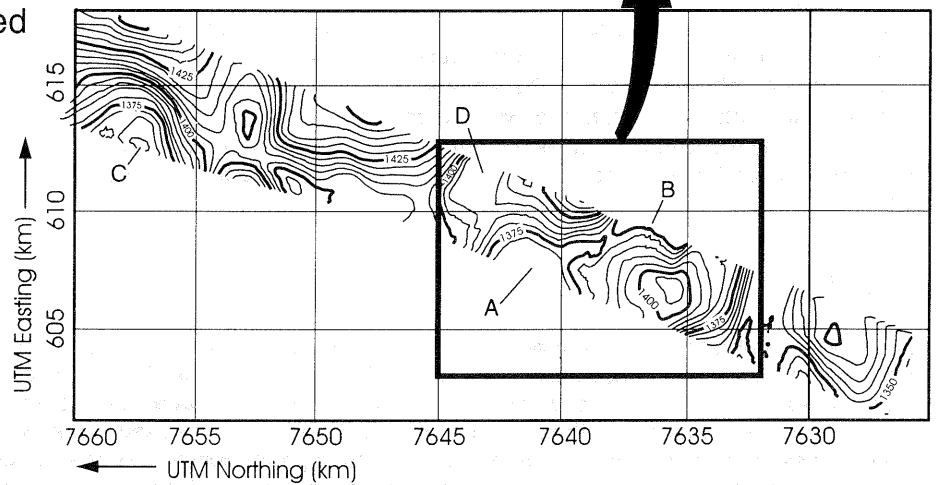
## REFERENCES

- Abshire, J. B., J. F. McGarry, L. K. Pacini, J. B. Blair, and G. C. Elman, 1994. Laser altimetry simulator, Version 3.0, User's Guide. *NASA Technical Memorandum 104588*, 66 page.
- Buften, J. L., 1989. Laser altimetry measurements from aircraft and spacecraft. *Proceedings of the IEEE*, Vol. 77, pp. 463-477.
- Csatho, B., T. F. Schenk, R. H. Thomas, and W. B. Krabill, 1995a. Topographic mapping by laser altimetry. *Proceedings of SPIE, Remote Sensing for Three-Dimensional Objects and Scenes*, ed. T. F. Schenk, Vol. 2572, pp. 10-20.
- Csatho, B., R. H. Thomas, 1995b. Determination of sea ice surface roughness from laser altimeter waveform. *BPRC Technical Report No-95-03*, Byrd Polar Research Center, The Ohio State University, Columbus, OH, 44 pages.
- Csatho, B. M., R. H. Thomas, and W. B. Krabill, 1995c. Mapping ice sheet topography with laser altimetry in Greenland (abstract). American Geophysical Union, 1995 Fall Meeting.
- Csatho, B., R. H. Thomas and W. B. Krabill, 1996. Mapping Ice Sheet Topography with Laser Altimetry in Greenland. *BPRC Technical Report No-96-01*, Byrd Polar Research Center, The Ohio State University, Columbus, OH, 53 pages.
- Echelmeyer, K., T. S. Clarke, and W. D. Harrison, 1991. Surficial glaciology of Jakobshavns Isbrae, West Greenland: Part I. Surface morphology. *Journal of Glaciology*, Vol. 37, No. 127, pp. 368-382.
- Fastook, J. L., H. H. Brecher, and T. J. Hughes, 1995. Derived bedrock elevations, strain rates, and stresses from measured surface elevations and velocities: Jakobshavns Isbrae, Greenland. *Journal of Glaciology*, Vol. 41, No. 137, pp. 161-173.
- Gardner, C. S., 1992. Ranging performance of satellite laser altimeters. *IEEE Transactions on Geoscience and Remote Sensing*, Vol. 30, pp. 1061-1072.
- Krabill, W. B., and R. N. Swift, 1985. Airborne lidar experiments at the Savannah River plant. *NASA Technical Memo, 4007*, 91 pages.
- Krabill, W. B., R. H. Thomas, C. F. Martin, R. N. Swift, and E. B. Frederick, 1995a. Accuracy of airborne laser altimetry over the Greenland ice sheet. *International Journal Remote Sensing*, Vol. 16, No. 7, pp. 1211-1222.
- Krabill, W., R. Thomas, K. Jezek, K. Kuivinen, and S. Manizade, 1995b. Greenland ice sheet thickness changes measured by laser altimetry. *Geophysical Research Letters*, Vol. 22, No. 17, pp. 2341-2344.
- Lindenberger, J., 1993. Laser-Profilmessungen zur topographischen Geländeaufnahme. *Ph. D. Dissertation, Deutsche Geodätische Kommission*, 131 pages.
- Thomsen, H. H., O. B. Olesen, R. J. Braithwaite and A. Weidick. 1989. Greenland ice-margin programme, a pilot study at Pakitsoq, northeast of Jakobshavns, central West Greenland. *Gronlands Geologiske Undersogelse, Rapport*, Vol. 145, 50-53.

a.) Aerial photograph



b.) Contour map derived from ATM data



c.) 3D view of DEM derived from ATM data

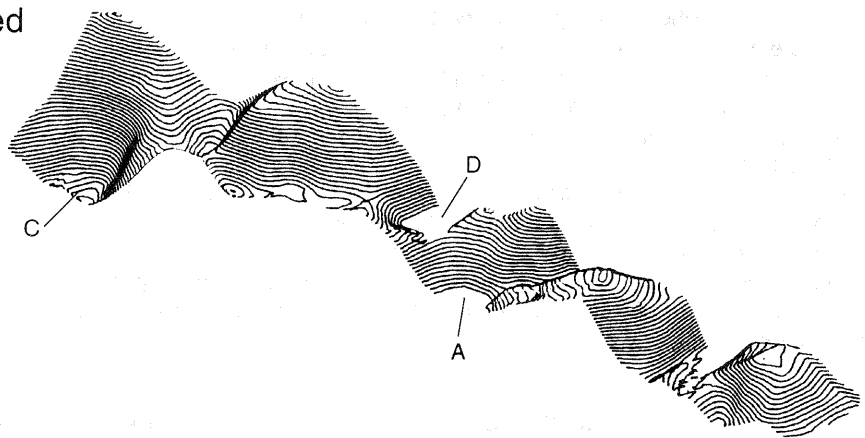


Figure 4: Comparison of laser altimetry and photogrammetrically derived elevations (Jakobshavns drainage basin, West Greenland). Lakes are labeled by capital letters. (a) Orthophoto with elevation contours derived from photogrammetry. (b) Contour map derived from laser altimetry. (c) Perspective view of DEM derived from laser altimetry.

*Aerial photographs provided by H. Brecher (OSU), photogrammetric measurements carried out by A. Templer (OSU)*